Korean J. Chem. Eng., **26**(4), 1155-1159 (2009)
DOI: 10.1007/s11814-009-0191-x

Sulfation diffusion model for SO_2 capture on the T-T sorbent at moderate temperatures

Yuran Li, Lizhai Yang, Changfu You, and Haiying Qi†

Key Laboratory for Thermal Science and Power Engineering of Ministry of Education,
Tsinghua University, Beijing 100084, P. R. China

(*Received 31 July 2008 • accepted 14 January 2009*)

Abstract−A sulfation model was developed for dry flue gas desulfurization (FGD) at moderate temperatures to describe the reaction characteristics of the T-T sorbent clusters and the fine CaO particles that fall off the sorbent grains in a circulating fluidized bed (CFB) reactor. The cluster model describes the calcium conversion and reaction rate for various size sorbent clusters. The sulfation reaction is first order with respect to the SO_2 concentration above 973 K. The calcium conversion and reaction rate for the CaO particles were obtained by extrapolation. In the model for CaO particle, the reaction rate is linearly related to the calcium conversion and the SO_2 concentration in the rapid reaction stage and linearly related only with the calcium conversion after the product layer forms. The sulfation model accurately describes the sulfation of the T-T sorbent flowing through a CFB reactor.

Key words: Sulfation Model, CaO Particle, Sorbent Cluster, Diffusion, Rreaction Rate

INTRODUCTION

Dry flue gas desulfurization (FGD) technology has been developed for moderate temperatures (673-1,073 K) using a circulating fluidized bed (CFB) reactor as a potential measure to reduce SO_2 emissions from coal-fired power plants in China.

The key to this technology is the T-T sorbent that is prepared by hydrating and drying a mixture of lime and fly ash, resulting in a large specific surface area and good pore structure. A high SO_2 removal rate of over 95% at a Ca/S ratio of 2 can be realized above 973 K [1]. The T-T sorbent with added industrial waste materials containing iron oxide can be used to simultaneously remove SO_2 and NO at 973-1,073 K [2].

The T-T sorbent particles flow through the CFB reactor as clusters due to adhesion and as fine CaO particles that have fallen off the sorbent grains, as shown in Fig. 1. Pilot-scale CFB tests showed more CaO in the bag filter ash than in the cyclone separator ash [3], which verifies that the CaO particles flake off the larger sorbent particles. The SO_2 diffuses within the clusters by inter-grain diffusion, inter-particle diffusion, and diffusion through the product layers. The diffusion in the CaO particles is only through the product layers.

A previously developed kinetic model for the SO_2 capture by the T-T sorbent [4] modeled the apparent reaction rate as a function of temperature and time based on the chemical reaction activation energy, E_a, and the activation energy for product layer diffusion, E_{diff}. However, that model did not completely describe the T-T sorbent diffusion processes because of the complex conditions in the CFB reactor. Other factors need consideration, such as the SO_2 concentration and the mass of the sorbent clusters.

Various methods are used to eliminate the inter-particle diffusion resistance to obtain kinetic data. A thin layer of $Ca(OH)_2$ was deposited onto a quartz glass plate to obtain a chemically controlled model to study the reaction rate and gas diffusion [5]. A small amount of $Ca(OH)_2$ was put into the 'net' sample-holder to give a variety of conditions to collect kinetic data from thermogravimetric data [6]. A differential fixed-bed reactor was also used to study the kinetics of the reaction between $Ca(OH)_2$/fly ash sorbent and SO_2 to develop a surface coverage model, which accurately describes the kinetics at low temperatures [7,8].

The aim of this work was to study the reaction rates for the various SO_2 diffusion processes by measuring the effects of the sorbent mass and the SO_2 concentration on the reaction rate. A T-T sorbent sulfation model was then developed for dry FGD at moderate temperatures.

PREPARATION OF SORBENT AND MEASUREMENTS

The T-T sorbent was prepared from lime and fly ash. The crushed lime particles were less than 20 mm in size and the fly ash particle size distribution ranged from 50 to 100 μm with a volumetric mean particle diameter of 73 μm. The lime and fly ash were slurried together with water for 2 h with a lime-to-fly ash mass ratio of 1 : 4, and dried at 423 K for 0.5-1 h.

The T-T sorbent grains had rough surfaces composed of pin-like and plate-like crystals at ambient temperature. When the sorbent grains were heated to 673 K, the crystals began to decompose to CaO as spherical particles as shown in Fig. 1(a) [4].

The experiments were performed in a thermogravimetric analyzer (TGA) that allows recording of the mass change of the solid reagent with time, with the mass increasing during the sulfation reaction. In this study, 5-50 mg samples for each run were spread on a 10 mm diameter sample pan. The sample was heated to the desired temperature, which caused the $Ca(OH)_2$ to decompose to CaO. The

---

† To whom correspondence should be addressed.
E-mail: hyqi@mail.tsinghua.edu.cn

‡ This work was presented at the 7th China-Korea Workshop on Clean Energy Technology held at Taiyuan, Shanxi, China, June 26-28, 2008.

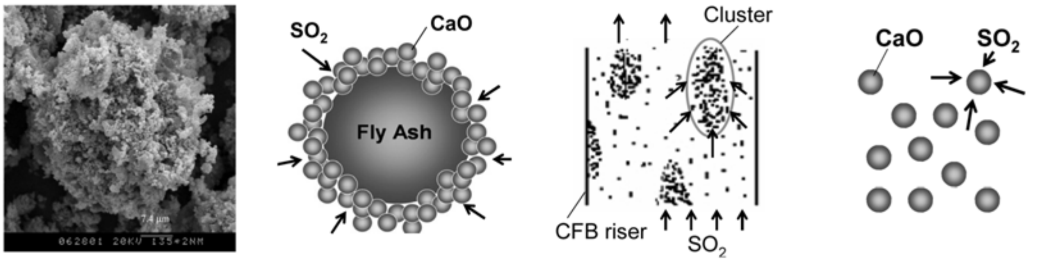

(a) SEM of a T-T sorbent grain

(b) Inter-particle diffusion for a sorbent grain

(c) Inter-grain diffusion for clusters

(d) Diffusion through product layers for a CaO particle

Fig. 1. Various kinds of SO$_2$ diffusion processes.

Table 1. Experimental conditions in the TGA reactor

Serial no.	T (K)	[O$_2$] (%)	[SO$_2$] (ppm)	N$_2$	m$_0$ (mg)
3.1	973	5	2,080	balance	5-50
3.2	973	5	620-3,950	balance	10 (±0.2)

reactive gas was then admitted to start the run.

The dry gas flow rate was 100 Ncm^{3}min^{-1}. The experimental conditions are shown in Table 1. No CO$_2$ was included in these experiments to avoid the interference between the sulfation and carbonation reactions [9].

After the mass change curves were recorded in each experiment, the calcium conversion curves were calculated by using the conversion expression:

$$x=\frac{m_t-m_0}{m_0\cdot\alpha}\cdot\frac{M_{CaO}}{M_{CaSO_4}-M_{CaO}} \tag{1}$$

Where x is the calcium conversion of the T-T sorbent, m_t is the sample mass which increases with time, m_0 is the initial dry sample mass, and α is the mass fraction of CaO in the sorbent. M_{CaO} is the molecular weight of CaO, and M_{CaSO_4} is the molecular weight of CaSO$_4$.

The reaction rate, r, is the derivative of the calcium conversion with respect to time:

$$r=\frac{dx}{dt} \tag{2}$$

RESULTS AND DISCUSSION

1. Effects of the Sorbent Mass

The conversion curves obtained by the TGA for various sorbent masses are presented in Fig. 2(a). The sulfation process has two obvious periods with the calcium conversion initially increasing rapidly and then more slowly later. There is a large amount of fresh CaO on the sorbent surface in the initial stage. After a product layer is generated, the diffusion resistance gradually increases with the product layer thickness. The conversion increases fast with time as the sorbent mass decreases. Thus, a given conversion will require longer times as the sorbent mass increases.

The effect of the sorbent mass on the reaction rate is shown in Fig. 2(b). As the sorbent mass decreases, the initial reaction rate increases but the reaction rate slows faster with time. Larger sorbent masses result in larger inter-particle diffusion resistances and smaller reaction rates, based on the assumption that the sorbent mass reflects the sorbent cluster size.

For a given SO$_2$ concentration, the increases in the absolute mass per minute are the same for the various sorbent masses; however, the changes of the relative mass, which is proportional to the conversion, are different.

As shown in Fig. 3, the time to reach a specific conversion is linearly related to the initial sorbent mass, m_0, as shown in Eq. (1). The fits in Fig. 3 have correlation coefficients of all 0.99; thus, the times can be related to the initial masses as:

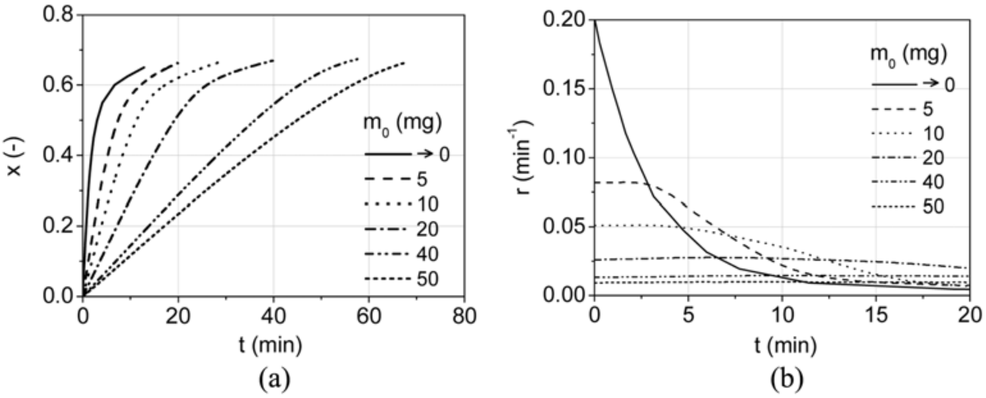

Fig. 2. Effects of sorbent mass on the calcium conversion (a) and reaction rate (b) (Conditions: T=973 K, [SO$_2$]=2,080 ppm, [O$_2$]=5%, N$_2$ balance, m$_0$=5-50 mg).

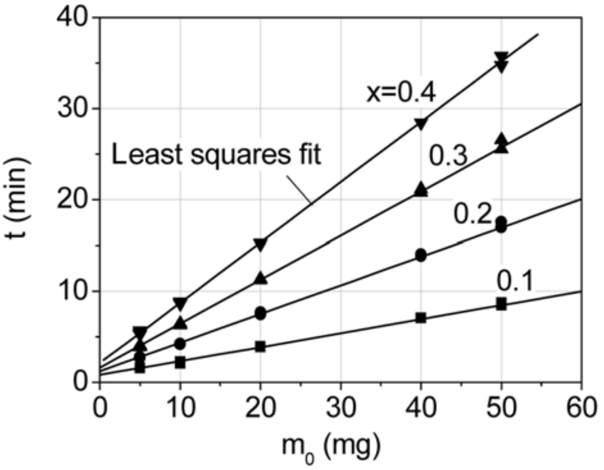

Fig. 3. Linear relationship between the reaction time and the initial mass for various conversions (Conditions: T=973 K, [SO_2]=2,080 ppm, [O_2]=5%, N_2 balance).

$$t=a+b\cdot m_0,\ (m_0\leq 50\ \text{mg}) \tag{3}$$

When m_0 is very small and trends to zero, bm_0 is far smaller than a; therefore, t≈a. A set of t–m_0 plots for various x (shown in Fig. 3) can then determine a set of values of a, which is the time for sorbent with $m_0\rightarrow 0$ to reach a given conversion; therefore, the relationship of x to a is the same as x to t and the relationship for r to a is the same as for r to t, as shown in Fig. 2.

The conversion for sorbent with $m_0\rightarrow 0$ increases much faster than conversions for larger sorbent masses. The initial reaction rate, 0.20 min^{-1}, is much larger than for 5 mg sorbent which is 0.08 min^{-1}.

The curve shape at $m_0\rightarrow 0$ (actually $m_0=0$) indicates that the physical effect at $m_0\rightarrow 0$ is a CaO particle flaking off the T-T sorbent surface. With CaO particles, the sulfation process involves diffusion through the product layer without inter-grain diffusion and inter-particle diffusion; therefore, the reaction rate is larger. However, the physical effect for $m_0\rightarrow 0$ does not reflect a CaO molecule, whose mass is much smaller than the CaO particle, since the molecular CaO reaction rate would be constant and not change with time. The reaction rate at $m_0\rightarrow 0$ was shown to decrease with time, in Fig. 2(b).

The relationship between b and x (Fig. 4) shows that b and x are related linearly with a correlation coefficient of 0.99; therefore,

$$b=c\cdot x,\ (x\leq 0.6) \tag{4}$$

Where c is a function of the SO_2 concentration. The linear relation between b and x holds up to x=0.6, which means that the diffusion has not reach the product layer diffusion controlled stage. At a given SO_2 concentration, c is the time for 1 mg sorbent to reach x=1. Therefore, this parameter can be used to estimate the minimum time required for the sorbent to convert completely.

Eqs. (3) and (4) can be rearranged to give:

$$t=a+c\cdot m_0\cdot x,\ (m_0\leq 50\ \text{mg}) \tag{5}$$

The conversion change with time of clusters with any initial mass can then be calculated from Eq. (5) for clusters up to 50 mg.

2. Sulfation Model for Sorbent Clusters

In Eq. (4), b is linearly related to x, and the slope, c, in Eqs. (4) and (5), decreases with increasing SO_2 concentration. The values of c for the three curves in Fig. 4 are 3.92, 1.78 and 1.23. The reciprocal of c is linearly related to the SO_2 concentration. Data for SO_2 concentrations of 1,040 ppm, 2,080 ppm and 3,950 ppm were collected to give:

$$\frac{1}{c}=2.21\times 10^{-4}\cdot C_{SO_2} \tag{6}$$

Eqs. (5) and (6) can then be combined to give the calcium conversion for clusters as a function of the initial mass, time and SO_2 concentration:

$$x=\frac{2.21\times 10^{-4}}{m_0}\cdot(t-a)\cdot C_{SO_2},\ \ (C_{SO_2}\leq 3.95\times 10^{-3}) \tag{7}$$

Therefore, Eq. (6) applies for SO_2 concentrations up to 3,950 ppm with the value of c given in Eq. (5). The special condition of m_0=0 will be analyzed further in the next section.

The reaction rate as a function of SO_2 concentration cannot be

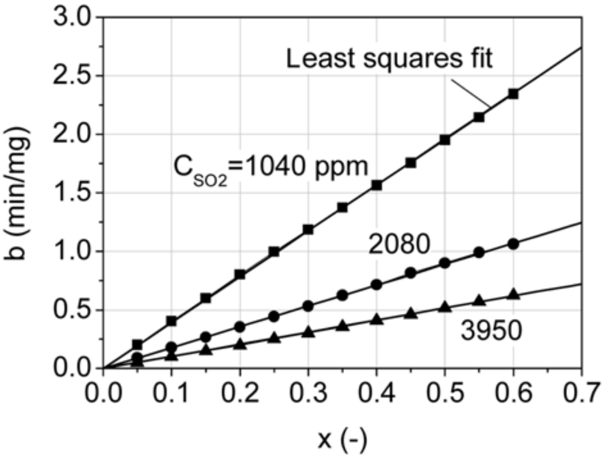

Fig. 4. Relationship between b and x at various SO_2 concentrations (Conditions: T=973 K, [SO_2]=1,040-3,950 ppm, [O_2]=5%, N_2 balance, m_0=5-50 mg).

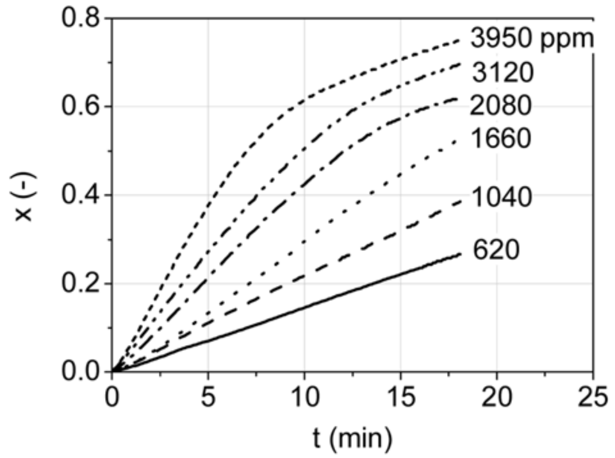

Fig. 5. Effects of SO_2 concentration on the conversion (Conditions: T=973 K, [SO_2]=620-3,950 ppm, [O_2]=5%, N_2 balance, m_0= 10 mg).

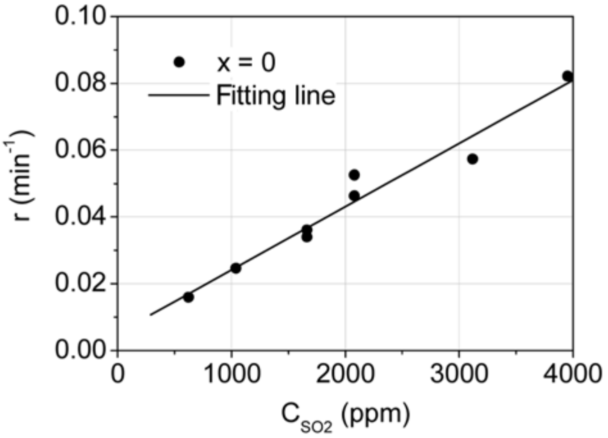

Fig. 6. Reaction rate for various SO_2 concentrations (Conditions: T=973 K, $[SO_2]$=620-3,950 ppm, $[O_2]$=5%, N_2 balance, m_0= 10 mg).

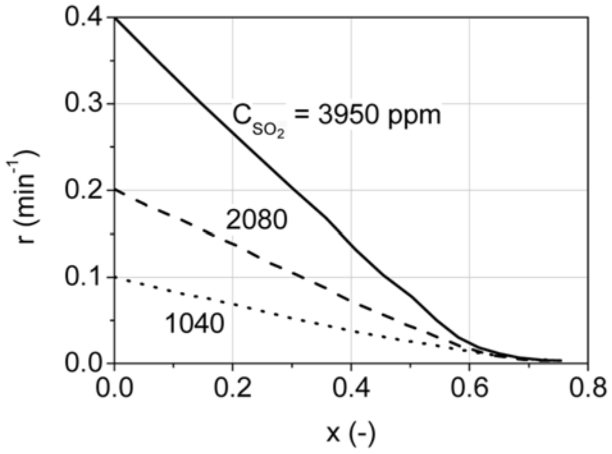

Fig. 7. Reaction rates for CaO particles at various SO_2 concentrations (Conditions: T=973 K, $[SO_2]$=1,040-3,950 ppm, $[O_2]$= 5%, N_2 balance).

deduced directly from Eq. (7), since a changes with x. Marsh et al. [5] showed that the sulfation reaction is first order in the SO_2 concentration in the presence of O_2 above 1,013 K. The effects of SO_2 concentration on the conversion were then studied with an initial sorbent mass of 10 mg at 973 K, with the results shown in Fig. 5.

The conversion and the slope of the curves in Fig. 5 both as the SO_2 concentration increase. Therefore, the reaction rate is significantly stronger at higher SO_2 concentrations. The relation between the reaction rate and the SO_2 concentration shown in Fig. 6 can be obtained by assuming that the initial (x=0) reaction rate is the maximum reaction rate.

The reaction rate in Fig. 6 varies linearly with the SO_2 concentration with a correlation coefficient of 0.98. This linear correlation means that the sulfation reaction is first order with respect to the SO_2 concentration. This apparent reaction order has been observed by other authors [10-12], so it can be concluded that the sulfation reaction is first order relative to the SO_2 concentration above 973 K. The reaction rate can be expressed as a function of the SO_2 concentration as:

$$r=k\cdot C_{SO_2}, \ (T\geq 973\ K,\ C_{SO_2}\leq 3.95\times 10^{-3}) \tag{8}$$

Further analysis has indicated that Eq. (8) can be applied for x≤ 0.6. Inter-particle diffusion will be present for 10 mg sorbent grains; therefore, the linear relationship between the reaction rate and the SO_2 concentration does not prove whether the chemical reaction or the diffusion is the rate controlling step in the rapid reaction stage.

A sulfation model for the T-T sorbent clusters was then developed for dry FGD at 973 K. The model is accurate for the SO_2 concentrations less than 3,950 ppm.

3. CaO Particle Sulfation Model

The special condition of $m_0 \rightarrow 0$ is analyzed in this section. The reaction rate for the CaO particles was obtained by extrapolation for various SO_2 concentrations to get the relationship between the reaction rate and conversion shown in Fig. 7. The reaction rate as a function of time can be used in a Lagrangian analysis; however, the reaction rate as a function of conversion is required for an Eulerian analysis.

The reaction process includes two stages with a critical point (x_{cr}) at about 0.6. Before the critical point, during the rapid reaction stage, the reaction rate is relatively high and is sharply influenced by the SO_2 concentration with higher SO_2 concentrations giving higher reaction rates. The reaction rate decreases linearly as the conversion increases. After the critical point, the product layer diffusion becomes the rate-controlling step, and the reaction rate as well as the effect of the SO_2 concentration both decrease as the conversion increases.

The curves for the different SO_2 concentrations almost overlap after the critical point. The critical point for CaO particles is slightly larger than for the 10 mg sorbent grains, because the gas diffusion in the particles and the grains cannot be avoided in the sorbent grains.

As the reaction continues, the product layer gradually covers the sorbent surface and the reaction rate tends to be controlled by the diffusion through the product layer. In this case, the product layer diffusion may be related to the ionic outward diffusion where the solid reactant migrates outward through the product layer by Ca^{2+} and O^{2-} ionic diffusion to react with the SO_2 and O_2 on the surface [13-15]. If the number of ions diffusing to the gas/$CaSO_4$ interface is less than the number of SO_2 molecules there, increases of the SO_2 concentration will not contribute much to the reaction rate.

The sulfation model for CaO particles based on these results with x_{cr}=0.6 is given by:

$$r=k_1\cdot C_{SO_2}\cdot(1-a_1x), \ (x\leq 0.6) \tag{9}$$

$$r=k_2\cdot(1-a_2x), \ (x>0.6) \tag{10}$$

$$k_1=k_{1,0}\exp\left(-\frac{E_a}{RT}\right), \ (973\ K\leq T\leq 1073\ K) \tag{11}$$

$$k_2=k_{2,0}\exp\left(-\frac{E_{diff}}{RT}\right), \ (973\ K\leq T\leq 1073\ K) \tag{12}$$

Before the critical point, the reaction rate is a first order function of the conversion and the SO_2 concentration. After the critical point, the reaction rate is only a function of the conversion.

In Eqs. (11) and (12), the reaction rate constant, k_1, is applied in the rapid reaction stage, while the diffusion rate constant, k_2, is applied after the product layer is completely generated. The chemical reaction activation energy, E_a, of 13.9 kJ/mol and the activation energy for the product layer diffusion, E_{diff}, of 49.3 kJ/mol were obtained previously [4]. At 973 K, $k_{1,0}$ is 5.57×10^{-4} $min^{-1}ppm^{-1}$ and $k_{2,0}$ is 21.3 min^{-1}. The other two parameters are a_1 equal to 1.61 and a_2 equal to 1.25.

In Eqs. (9) and (10), the reaction rate is proportional to the conversion. Similar equations have been used in the surface coverage model that describes the reaction between $Ca(OH)_2$ or $Ca(OH)_2$/fly ash sorbent and SO_2 at low temperatures [7,8]. Similar equations obtained from the pore-plugging model have been used to analyze the sulfation of limestone at high temperatures [16].

The sulfation model for CaO particles expressed by Eqs. (9)-(12) gives the reaction rate as a function of T, x and C_{SO_2}. The model can be used for 973-1,073 K as the parameters, x_{cr}, $k_{1,0}$, $k_{2,0}$, a_1 and a_2 change with temperature. The critical point, x_{cr}, ranges from 0.6 to 0.65.

The sulfation model describes the sulfation of CaO particles in CFB reactor. The other components in the flue gas, such as CO_2 and NO_x, will also affect the reaction, so the sulfation model needs further improvement before used in numerical simulations of desulphurization.

CONCLUSIONS

The sorbent cluster mass greatly influences the calcium conversion and reaction rate in desulfurization processes. A sulfation model for sorbent clusters was developed as a function of the time, SO_2 concentration and initial mass. The model describes the calcium conversion and reaction rate for sorbent clusters with different masses. The sulfation reaction is first order with respect to the SO_2 concentration for conversion less than about 0.6 above 973 K.

The calcium conversion and reaction rate for CaO particles was then obtained by extrapolation. A sulfation model for CaO particles was developed in which the reaction rate is a linear function of the calcium conversion and SO_2 concentration before the dense product layers form and is a linear function of the calcium conversion after the product layers form.

ACKNOWLEDGMENT

This work was supported by the National Basic Research Program of China (973 Program) No. 2006CB200305.

NOMENCLATURE

a : fit parameter in Eq. (3) [min]
a_1, a_2 : constants in Eqs. (9) and (10) [-]
b : fit parameter in Eq. (3) [min/mg]
c : fit parameter in Eq. (4) [min/mg]
C_{SO_2} : SO_2 concentration [ppm]
E_a : chemical reaction activation energy [kJ/mol]
E_{diff} : activation energy for product layer diffusion [kJ/mol]
k : fit parameter in Eq. (8) [1/(min ppm)]
k_1 : reaction rate constant [1/(min ppm)]
k_2 : diffusion rate constant [1/min]
$k_{1,0}$: pre-exponential factor [1/(min ppm)]
$k_{2,0}$: pre-exponential factor [1/min]
m_0 : initial mass of sorbent sample [mg]
m_t : mass increment during reaction in TGA [mg]
r : reaction rate [1/min]
R : gas constant, [J/(mol K)]
t : reaction time [min]
T : reaction temperature [K]
x : calcium conversion [-]
a : mass fraction of CaO in T-T sorbent [-]

REFERENCES

1. B. Hou, H. Y. Qi, C. F. You and X. C. Xu, *Energy Fuels*, **2**, 73 (2005).
2. T. J. Li, Y. Q. Zhuo, J. Y. Lei and X. C. Xu, *Korean J. Chem. Eng.*, **24**, 1113 (2007).
3. J. Zhang, C. F. You, S. W. Zhao, C. H. Chen and H. Y. Qi, *Environ. Sci. Technol.*, **42**, 1705 (2008).
4. Y. R. Li, H. Y. Qi, C. F. You and X. C. Xu, *Fuel*, **86**, 785 (2007).
5. D. W. Marsh and D. L. Ulrichson, *Chem. Eng. Sci.*, **40**, 423 (1985).
6. I. Fernández, A. Garea and A. Irabien, *Fuel*, **77**, 749 (1998).
7. C. F. Liu and S. M. Shih, *J. Chin. Inst. Chem. Engrs.*, **33**, 407 (2002).
8. C. F. Liu, S. M. Shih and R. B. Lin, *Ind. Eng. Chem. Res.*, **43**, 4112 (2004).
9. C. S. Ho, S. M. Shih and C. D. Lee, *Ind. Eng. Chem. Res.*, **35**, 3915 (1996).
10. H. Kim and D. Park, *Korean J. Chem. Eng.*, **4**, 143 (1987).
11. Q. Zhong., *Thermochimica Acta*, **260**, 126 (1995).
12. H. Liu, S. Katagiri, U. Kaneko and K. Okazaki, *Fuel*, **79**, 945 (2000).
13. C. Hsia, G. R. Saint Pierre, K. Raghunathan and L. S. Fan, *AIChE J.*, **39**, 698 (1993).
14. C. Hsia, G. R. Saint Pierre and L. S. Fan, *AIChE J.*, **41**, 2337 (1995).
15. Y. Z. Li, H. L. Tong, Y. Q. Zhuo, C. H. Chen and X. C. Xu, *Environ. Sci. Technol.*, **40**, 4306 (2006).
16. D. C. Lee and C. Georgakis, *AIChE J.*, **27**, 472 (1981).